






Model Based Identification of the Measured Vibration Multi-fault Diagnostic Signals Generated by a Large Rotating Machine

Tomasz Szolc^(✉) , Robert Konowrocki , and Dominik Pisarski 

Institute of Fundamental Technological Research of the Polish Academy of Sciences,
Ul. Pawińskiego 5B, 02-106 Warsaw, Poland
tszolc@ippt.pan.pl

Abstract. Large rotating machines are usually affected by more or less severe vibrations excited simultaneously by various manufacturing errors and operational defects. In order to identify the causes of these adverse effects on the basis of measured diagnostic signals registered during a regular operation, it is necessary to obtain a theoretical basis regarding possible dynamic responses of the monitored machine to its most likely failures. This paper shows how to achieve this target on the example of monitoring results of a large blower used in the mining industry. In the advanced structural hybrid model of the rotor shaft system of this blower, in addition to the impact of static unbalance, there is included simultaneous interaction of dynamic unbalance of the blower overhung rotor, parallel and angular misalignments of the shaft sections, inner anisotropy of the couplings, pressure pulsation of the working medium caused by incorrect stagger angles of the blower rotor blades, and electromagnetic pull of rotors of the driving electric motors. The contribution of the above-mentioned imperfections to the dynamic behavior of the system will be identified by means of a multi-fault model-based identification method using the harmonic excitation approach, where vibratory motions are described in the space of modal coordinates and malfunction effects are modelled by the use of equivalent external loadings. Computational examples will be devoted to demonstrating the influence of a faulty setting of the stagger angles of the blower blades on lateral vibrations of the entire rotating system with the simultaneous influence of the aforementioned imperfections.

Keywords: Rotor Machine · Model-Based Multi-Fault Identification · Monitoring of Vibration Signals · Rotor-Shaft Hybrid Model with Imperfections

1 Introduction

Many manufacturing and operational defects of modern rotating machines are the cause of various types of vibrations of these objects. Such oscillations, on the one hand, can pose a serious threat to the correct operation of these machines, but on the other hand, these vibrations can be used to identify the above-mentioned defects. The most common imperfections in rotor-shaft systems of rotating machines include residual static and

dynamic unbalances, mutual parallel and angular misalignments of rotor-shaft segments connected by couplings or joints, internal anisotropy of these shafts and couplings connecting them, shaft bows and transverse cracks, rotor-stator rub impact, various types of damages of bearings supporting these shafts and many others. The imperfections listed above are most often the cause of bending/lateral vibrations of the rotor-shaft systems of these machines. In contrast to the often occurring torsional and axial vibrations of shaft lines of the rotating machines, bending/lateral oscillations are relatively easy to measure using sensors usually mounted on housings of rotor-shaft bearing supports. Therefore, monitoring of these vibrations and proper processing of the measurement signals generated by these oscillations can be a source of valuable diagnostic information enabling an effective identification of the above-mentioned defects affecting the majority of typical rotating machines.

According to the above, the problem of identifying defects in rotating machines has been an ambitious research challenge for the last few decades, engaging many outstanding researchers from leading scientific and industrial centers around the world to solve it. Apart from diagnosing the condition of a given machine, basing on the current monitoring of its vibrations, an extremely important aspect that was and still is an investigation of the sensitivity of this machine to excitations of certain types of vibrations by certain types of imperfections in its rotor-shaft system.

Analyses of bending/lateral vibrations of rotating systems induced by unbalances, mainly static, are already a classic in the field of dynamics of rotating machines, which is reflected in numerous monographs, such as in [1, 2]. Recently, studies of the impact of transverse cracks in rotor shafts have gained a similar rank, as evidenced by so many publications, even an attempt to select the most representative ones is extremely difficult. Although the phenomenon of various cases of parallel and angular misalignments of shafts and rotors has been observed since the beginning of the drive systems of various types of machines, devices and vehicles, scientific research on these imperfections was intensified at the very end of the 20th century and especially in the two decades of the current century. This is confirmed by numerous publications from that period, for example [3–8].

Based on reviews of the available literature, it can be concluded that the problem of inner anisotropy of the dynamic properties of rotor systems has not been fully investigated so far. The inner anisotropy of rotor shafts, distributed continuously along their length, was investigated by means of the finite element method for cognitive purposes in the dissertation [9], and for the diagnosis of imperfections in [7]. Different values of shaft stiffness in mutually perpendicular directions to the axis of rotation as a result of a transverse crack in a given rotor shaft section, as e.g., in [10–13], or as a consequence of bad coupling assembly can be considered as the local anisotropy, which was the subject of research in [14]. It should be noted that in the above-mentioned work [7], a synthetic summary of theoretical models of the types of faults considered here was made, where the sensitivity of the rotor-shaft system to these imperfections acting simultaneously was examined by treating them as effects with stochastically distributed uncertain parameters. The sensitivity of the rotor-shaft system to the simultaneous action of the defects under consideration was also analyzed in [14], where an interval approach was used to take into account the uncertainty of parameters of these imperfections.

With regard to examination of the sensitivity of rotor-shaft systems to various types of imperfections using various methods, their identification from the viewpoint of the fundamentals of the dynamics of mechanical systems boils down to solving the so-called inverse problems. Due to the great importance of this issue, many methods have been developed over the past two decades to identify faults in machines, including rotating machines, based on measured vibrations induced by these imperfections. In the work [15], the most important methods of fault identification applied in machines, vehicles and flying objects were classified. In turn, in the typical review paper [16], advantages and disadvantages of various commonly used methods for identifying defects in rotating machines are specified. Based on the considerations made in these works, as well as in the papers [10, 11], the fault identification methods based on recorded vibration signals can be divided into two main groups: The first one includes statistical methods that use empirically collected cause-and-effect relationships, where stochastic approaches, neural networks, fuzzy clusters and various methods of transformation of measured vibration time courses are most often used to guess the type of defect, its location and magnitude estimation. The second group includes methods based on physical and mathematical models of the vibrating objects themselves, in our case – the rotor-shaft systems, and on models of particular types of imperfections affecting these objects. It should be remembered that, in contrast to the methods belonging to the first group, the model-based fault identification methods require the most accurate knowledge of technical parameters and dynamic properties of the tested vibrating object and the development of a reliable theoretical model of it. The advantages of this group of identification methods were emphasized, among others in the work [16], justifying them with the use of physical fundamentals of the vibrating objects under study and the analyzed dynamic processes.

Identification of defects in rotor-shaft systems using model-based methods can be carried out in a variety of ways. For example, in the works [10, 11] and [17], simultaneously interacting different imperfections are localized and identified, which have been interpreted as external forces exciting bending/lateral vibrations of the rotor-shaft line of a steam turbogenerator. The inverse problem for unbalanced systems of rotor shafts with a transverse crack was solved in [12, 13] by means of stochastic methods using the results of Monte-Carlo simulations of coupled bending-torsional-longitudinal vibrations of the tested objects. In turn, in [18], a regression approach was applied to solve the inverse problem to identify simultaneously acting various defects by the use of a model of rigid rotors. The cause-and-effect relationships resulting from an operation of individual types of imperfections were collected by means of numerical simulations carried out in [19] using the structural FEM model of the rotor system. Then, they could be used to identify these defects by analyzing Fourier, wavelet and Hilbert-Huang transformations of time courses of bending/lateral vibrations recorded on the real object. However, in the work [20], a transverse crack of an unbalanced rotor shaft with misalignments was identified theoretically and experimentally by observation in the time domain of transient resonances under unsteady operating conditions.

Many model-based multi-fault identification methods enable more or less effective determination of the type of defect, estimation of its magnitude, and even localization. However, the majority of them require results of dynamic responses of the rotor-shaft system registered at variable rotational speed, as in [19, 20], e.g., in the conditions of

start-ups or run-downs of the machine, at several rotational speed values, [10, 11, 18], and even for opposite directions of these speeds, as in [18]. But it should be remembered that obtaining such results is not always possible, especially in the conditions of continuous operation of a given rotating machine working at a constant, e.g., nominal, rotational speed. And just such a case of operation of a real rotor machine will be considered in the presented paper.

Namely, the subject of research will be the model-based multi-fault identification carried out for a high-power blower used in the mining industry. The main purpose of considerations performed in this work is the current assessment of the condition of the rotor-shaft system of this machine by means of the detection and identification of simultaneously affecting faults during its normal operation. The most likely types of imperfections are considered to be static and dynamic unbalance of the overhung rotor of this blower, static unbalances of the drive motor rotors, parallel and angular misalignment of the shaft segments, internal anisotropy of the couplings and excessive pulsation of the blower working medium causing additional vibrations of the entire rotor-shaft system. It should be emphasized that the above-mentioned types of imperfections should be considered the most probable due to structure properties of this object and the way of manufacturing and mutual assembly of its elements. Identification of these defects will be carried out on the basis of current measurements of lateral vibrations of bearing housings recorded in steady-state, nominal machine operating conditions.

2 Modelling of the Blower Rotor-Shaft System with Imperfections

The object of considerations in this paper is a heavy industrial blower driven by two asynchronous motors mutually connected in series with a power of 3.55 MW each at the rated speed of 992 rpm. The scheme of the rotor-shaft system of this machine is shown in Fig. 1. The drive shaft of this blower is driven by the motors via two lamella couplings C1 and C2 interconnected by an intermediate shaft, and the motors are connected with each other via two lamella couplings C3 and C4. The rotor of this blower is characterized by the outer diameter of 4.6 m and the total mass 5.74 times greater than the mass of its drive shaft. This shaft is suspended on two oil-journal bearings #1 and #2 mutually distant by 0.81 m. The spans of the rolling element bearings #3 – #4 and #5 – #6 supporting the both motor rotors are equal to 1.76 m.

Taking into account the structure of the entire drive system of this blower and the results of the routine, ongoing monitoring of the condition of the machine, the most probable imperfections affecting it are a static and dynamic unbalance of the blower rotor, static unbalance of the rotors of both drive motors, parallel and angular misalignments of all four lamellar couplings C1, C2, C3 and C4, an internal anisotropy of these couplings and a possibility of wrongly set-up stagger angles of selected blades of the blower rotor causing unfavorable pulsation of the working medium, which results in excitation of additional dangerous lateral vibrations.

In order to perform an effective multi-fault identification of the above-mentioned types of imperfections, it is necessary to adopt a suitably reliable and computationally efficient physical and mathematical model of the tested object. To achieve this goal, a hybrid model will be used, the structure of which is analogous to the commonly used

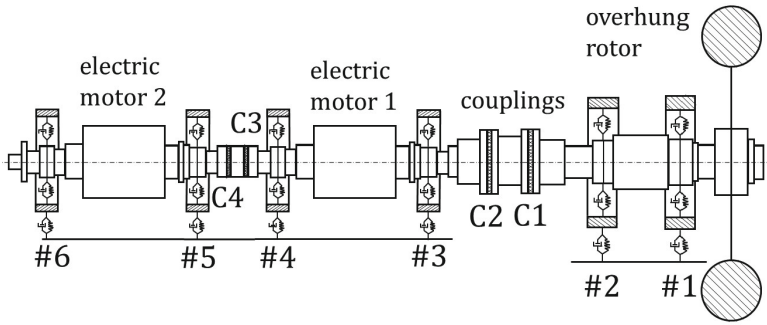


Fig. 1. Scheme of the rotor-shaft system of the industrial blower.

beam finite element models of rotor shaft systems. Namely, the hybrid model differs from the analogous FEM model in that the individual cylindrical segments of real rotor shafts are not discretized, but they are treated naturally as finite beam macro-elements with continuously distributed viscous-inertial-elastic properties. In this model, the flexural motion of cross-sections of each viscoelastic continuous macro-element is governed by the partial differential equation derived using the Rayleigh or Timoshenko rotating beam theory. Such equations contain gyroscopic forces mutually coupling rotor-shaft bending vibrations in the horizontal and vertical plane. The analogous coupling effect caused by the system rotational speed dependent shaft material damping, described by the use of the standard body model, is also included. With an accuracy that is sufficient for practical purposes, in the proposed hybrid model of the rotor-shaft system, some heavy rotors or coupling disks can be represented by rigid bodies attached to the macro-element extreme cross sections, as shown in Fig. 2a. Each bearing support is represented by the use of a dynamic oscillator of two degrees of freedom, where apart from the oil-film or rolling element interaction, also the visco-elastic properties of the bearing housing and foundation are taken into consideration, see Fig. 2b. This bearing model makes it possible to represent with relatively high accuracy kinetostatic and dynamic anisotropic and anti-symmetric properties of the oil-film or rolling elements in the form of constant or variable stiffness and damping coefficients.

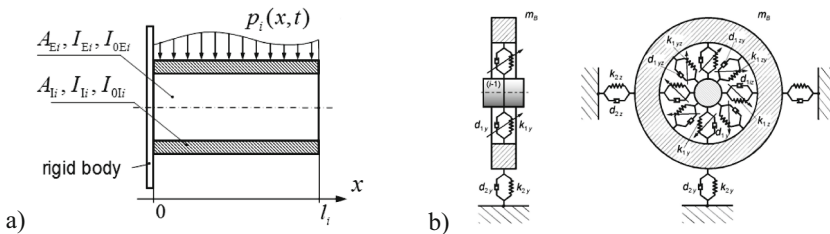


Fig. 2. The continuous finite macro-element a), the oscillator representing a bearing support b).

As in the works [12–14, 21], mutual connections of the successive macro-elements creating the stepped shaft as well as their interactions with the bearing supports and

rigid bodies representing the heavy rotors are described by equations of compliance conditions. These are the equations of geometrical conditions of equality for translational and rotational displacements of extreme cross-sections of the continuous macro-elements $x = L_i = l_1 + l_2 + \dots + l_{i-1}$ of the adjacent $(i - 1)$ -th and the i -th elastic macro-elements:

$$v_{i-1}(x, t) = v_i(x, t), \quad \frac{\partial v_{i-1}(x, t)}{\partial x} = \frac{\partial v_i(x, t)}{\partial x}, \quad (1)$$

where $v_i(x, t) = u_i(x, t) + jw_i(x, t)$, $u_i(x, t)$ being the lateral displacement in the vertical direction and $w_i(x, t)$ the lateral displacement in the horizontal direction, and j denotes the imaginary number. The second group of compliance conditions are dynamic ones, which generally contain linear, parametric and nonlinear equations of equilibrium for concentrated external forces, static and dynamic unbalance forces and moments, inertial, elastic and external damping forces, support reactions and gyroscopic moments. For example, the dynamic compliance conditions formulated for the rotating Rayleigh beam, and describing a simple connection of the mentioned adjacent $(i - 1)$ -th and the i -th elastic macro-elements, have the following form:

$$\begin{aligned} -m_i \frac{\partial^2 v_i}{\partial t^2} + EI_i \frac{\partial^3 v_i}{\partial x^3} - \rho I_i \frac{\partial^3 v_i}{\partial x \partial t^2} - EI_{i-1} \frac{\partial^3 v_{i-1}}{\partial x^3} + \rho I_{i-1} \frac{\partial^3 v_{i-1}}{\partial x \partial t^2} + \\ + j\Omega(t) \rho I_{0i} \frac{\partial^2 v_i}{\partial x \partial t} - j\Omega(t) \rho I_{0,i-1} \frac{\partial^2 v_{i-1}}{\partial x \partial t} = Y_i(t), \quad (2) \\ -J_i \frac{\partial^3 v_i}{\partial x \partial t^2} + EI_i \frac{\partial^2 v_i}{\partial x^2} - EI_{i-1} \frac{\partial^2 v_{i-1}}{\partial x^2} + j\Omega(t) J_{0i} \frac{\partial^2 v_i}{\partial x \partial t} = Z_i(t), \end{aligned}$$

where the symbols m_i , J_i denote respectively the mass and diametric mass moment of inertia of the rigid disk, I_i and I_{0i} are the cross-sectional diametric and polar geometric moments of inertia, E , ρ denote the shaft material constants, $\Omega(t)$ is the current average, i.e., corresponding to rigid body motion, shaft rotational speed, $Y_i(t)$ and $Z_i(t)$ denote the concentrated external excitations in the form of transverse force and bending moment, respectively, $i = 1, 2, \dots, n$, and n is the total number of macro-elements in the hybrid model. By means of the dynamic compliance conditions there are described shaft interactions with discrete oscillators representing shaft bearing supports. As it follows from [12, 13], such compliance conditions contain anti-symmetrical terms with cross-coupling oil-film stiffness components, which couple shaft bending vibrations in two mutually perpendicular planes. In these equations the stiffness and damping coefficients can be constant or variable, where non-linear properties of the oil-film are taken into consideration.

The mathematical model of the coupling with an inner anisotropy and characterized also by the parallel and angular misalignment comes down to a description of the connection of the extreme cross-section of the rotating Rayleigh or Timoshenko beam, representing in this model the k -1-st coupling flange, with the extreme cross-section of the analogous beam, representing the k -th flange, by means of a massless spring with the given shear stiffness G_{0k} and bending stiffness H_{0k} . This description is a condition of equilibrium for viscoelastic, inertial and gyroscopic transverse forces and bending moments, which in the case of applying the Rayleigh beam bending theory takes the

following form containing concentrated harmonic excitations oscillating with a single-1X and double-synchronous 2X frequency:

$$\begin{aligned}
 & -EI_{k-1} \left(1 + e \frac{\partial}{\partial t} \right) \frac{\partial^3 v_{k-1}(x, t)}{\partial x^3} + \rho I_{k-1} \frac{\partial^3 v_{k-1}(x, t)}{\partial x \partial t^2} - 2j\Omega(t) \rho I_{k-1} \frac{\partial^2 v_{k-1}(x, t)}{\partial x \partial t} - \\
 & \quad - \left(G_{0k} + G_{Vk} e^{j(2\Theta(t) - \Delta_k)} \right) \cdot (v_{k-1}(x, t) - v_k(x, t) + D_k(\Theta(t) - \Psi_k)) = 0, \\
 & EI_k \left(1 + e \frac{\partial}{\partial t} \right) \frac{\partial^3 v_k(x, t)}{\partial x^3} - \rho I_k \frac{\partial^3 v_k(x, t)}{\partial x \partial t^2} + 2j\Omega(t) \rho I_k \frac{\partial^2 v_k(x, t)}{\partial x \partial t} + \\
 & \quad + \left(G_{0k} + G_{Vk} e^{j(2\Theta(t) - \Delta_k)} \right) \cdot (v_{k-1}(x, t) - v_k(x, t) + D_k(\Theta(t) - \Psi_k)) = 0, \\
 & EI_{k-1} \left(1 + e \frac{\partial}{\partial t} \right) \frac{\partial^2 v_{k-1}(x, t)}{\partial x^2} + \left(H_{0k} + H_{Vk} e^{j(2\Theta(t) - \Gamma_k)} \right) \\
 & \quad \cdot \left(\frac{\partial v_{k-1}(x, t)}{\partial x} - \frac{\partial v_k(x, t)}{\partial x} - F_k(\Theta(t) - \Phi_k) \right) = 0, \\
 & EI_k \left(1 + e \frac{\partial}{\partial t} \right) \frac{\partial^2 v_k(x, t)}{\partial x^2} + \left(H_{0k} + H_{Vk} e^{j(2\Theta(t) - \Gamma_k)} \right) \\
 & \quad \cdot \left(\frac{\partial v_{k-1}(x, t)}{\partial x} - \frac{\partial v_k(x, t)}{\partial x} - F_k(\Theta(t) - \Phi_k) \right) = 0 \quad \text{for } x = \sum_{i=1}^{k-1} l_i.
 \end{aligned} \tag{3}$$

Here, the all symbols above have been already defined for relationships (2), and the explicit time functions of the shaft current rotation angle $\Theta(t)$, which occur in (3), i.e., $D_k(\Theta(t) - \Psi_k)$, $F_k(\Theta(t) - \Phi_k)$ and $C \cdot \exp(j(2\Theta(t) - \mathcal{E}_k))$, where $C = G_{Vk}$ or H_{Vk} and $\mathcal{E}_k = \Delta_k$ or Γ_k , can be treated as concentrated external excitations applied to both flanges of the coupling.

3 Mathematical Solution of the Problem

The complete mathematical formulation and solution for the rotor-shaft system hybrid model applied here can be found e.g., in [21] and [12, 13]. Namely, the solution for simulations of the forced lateral vibrations has been obtained using the analytical–computational approach described in the papers mentioned above. In the first step, by solving the differential eigenvalue problem for the linear orthogonal system, the set of bending eigenmode functions is determined. Next, all anti-symmetric, gyroscopic and parametric terms omitted to solve the eigenvalue problem are regarded here as response-dependent external excitations. Finally, for the hybrid model of the rotor-shaft system, the Fourier solution in the form of series in the orthogonal eigenfunctions is applied in the following form for the each i -th macro-element:

$$v_i(x, t) = \sum_{m=1}^{\infty} V_{im}(x) \xi_m(t), \quad i = 1, 2, \dots, n, \tag{4}$$

where $V_{im}(x) = U_{im}(x) + jW_{im}(x)$ denote the orthogonal complex eigenfunctions and $\xi_m(t)$ are the unknown modal coordinates. Here, the eigenfunction real part $U_{im}(x)$ corresponds to rotor-shaft lateral displacements in the vertical plane and the imaginary part $W_{im}(x)$ corresponds to lateral displacements in the horizontal plane. This approach leads generally to an infinite number of known separate ordinary differential equations in modal coordinates. But, in the case considered here, the above mentioned response-dependent external excitations and gyroscopic forces mutually couple these equations. Thus, consequently and similarly as in [14] one obtains the following set of parametric ordinary differential equations in the modal coordinates:

$$\mathbf{M}_0 \ddot{\mathbf{r}}(t) + \mathbf{D}(\Omega) \dot{\mathbf{r}}(t) + [\mathbf{K}(\Omega) + \mathbf{K}_a(\exp(j2\Theta(t)))] \mathbf{r}(t) = \mathbf{F}(\Omega^2, \Theta(t)), \quad (5)$$

where: $\mathbf{D}(\Omega) = \mathbf{D}_0 + \mathbf{D}_g(\Omega)$ and $\mathbf{K}(\Omega) = \mathbf{K}_0 + \mathbf{K}_b + \mathbf{K}_d(\Omega)$, $\Theta(t) = \int_0^t \Omega(\tau) d\tau$.

The symbols \mathbf{M}_0 , \mathbf{K}_0 are the diagonal modal mass and stiffness matrices, respectively, \mathbf{K}_a is the symmetrical matrix of parametric excitation with a double-synchronous frequency $2X$ due to anisotropic properties of the couplings, \mathbf{D}_0 denotes the symmetrical damping matrix and $\mathbf{D}_g(\Omega)$ is the skew-symmetrical matrix of gyroscopic effects. Skew- or non-symmetrical elastic properties of the bearings are expressed by matrix $\mathbf{K}_b(\Omega)$. Anti-symmetrical effects due to the standard body material damping model of the rotating shaft are described by the skew-symmetrical matrix $\mathbf{K}_d(\Omega)$. The symbol $\mathbf{F}(\Omega^2(t), \Theta(t))$ denotes the vector of external excitations. The modal coordinate vector $\mathbf{r}(t)$ consists of the unknown time functions $\xi_m(t)$ standing in the Fourier solution (4). The mathematically proven quick convergence of the Fourier solution allows for limiting the number of Eqs. (5) to solve to the number of bending eigenmodes taken into consideration in the frequency range of interest.

4 Modelling of the Rotor-Shaft System Imperfections

As mentioned above, the identification of faults in the rotor-shaft system of the blower under consideration can be carried out only in steady-state, nominal conditions of its operation. Owing to this, relations (1)–(3) and (5) can be solved for $\Omega(t) = \Omega = \text{const}$. Similarly to the papers [10, 11, 17], it was assumed that the bending/lateral vibrations of the tested system are induced by time-varying forces and moments caused by the imperfections sought. In the further considerations, the horizontal (marked with upper indices “H”) and vertical components (marked with upper indices “V”) of these forces and moments will constitute dynamic models of individual types of the most probable imperfections expected in the object under study. These are:

1. Static unbalances of the rigid rotor-disks with masses m_i and eccentricities ε_i :

$$Y_i^H(t) = m_i \varepsilon_i \Omega^2 \cos(\Omega t - \alpha_i), \quad Y_i^V(t) = m_i \varepsilon_i \Omega^2 \sin(\Omega t - \alpha_i), \quad (6a)$$

where α_i are the unbalance phase angles;

2. Static unbalances of the cylindrical shaft segments with unit masses ρA_i and eccentricities e_i :

$$y_i^H(t) = \rho A_i e_i \Omega^2 \cos(\Omega t - \beta_i), \quad y_i^V(t) = \rho A_i e_i \Omega^2 \sin(\Omega t - \beta_i), \quad (6b)$$

where β_i are the unbalance phase angles;

3. Dynamic unbalances of the i -th rigid rotor-disks, [14]:

$$\begin{aligned} z_i^H(t) &= \Omega^2 \left[\frac{1}{2} (I_{\xi i} - I_{\eta i}) \sin(2\alpha_i) \right] \cos(\Omega t - \delta_i), \\ z_i^V(t) &= \Omega^2 \left[\frac{1}{2} (I_{\xi i} - I_{\eta i}) \sin(2\alpha_i) \right] \sin(\Omega t - \delta_i), \end{aligned} \quad (6c)$$

where $I_{\xi i}, I_{\eta i}$ are the two out of three central, main mass moments of inertia of the rigid disk, α_i denote the small angles of rotation of its central principal axes of inertia with respect to the disk centre of mass, so that one of these axes does not coincide with the axis around which this disk rotates, and δ_i are the unbalance phase angles;

4. Parallel misalignments of the k -th coupling, [3, 5–8, 14]:

$$D_k^H(t) = G_{0k} \delta_k \cos(\Omega t - \Psi_k), \quad D_k^V(t) = G_{0k} \delta_k \sin(\Omega t - \Psi_k), \quad (6d)$$

where G_{0k} denotes the lamella coupling shear stiffness, δ_k is the mutual shaft misalignment off-set and Ψ_k denotes the parallel misalignment phase angle;

5. Angular misalignments of the k -th coupling, [7, 8, 14]:

$$F_k^H(t) = F_{0k} \beta_k \cos(\Omega t - \Phi_k), \quad F_k^V(t) = F_{0k} \beta_k \sin(\Omega t - \Phi_k), \quad (6e)$$

where F_{0k} denotes the lamella coupling bending stiffness, β_k is the angular misalignment due to a coupling flange machining error and Φ_k denotes the angular misalignment phase angle.

It should be noted that all forces exciting vibrations, which result from the types of imperfections listed above and follow from physical fundamentals and practical observations, oscillate harmonically in time with a synchronous frequency of 1X.

6. Inner anisotropy of the couplings:

The local inner anisotropy of the couplings is the cause of parametric effects in the adopted hybrid model, which was expressed in the system of Equations (5) by the components of the stiffness matrix fluctuating with a double synchronous frequency of 2X. Since these effects are analogous to the effects of the occurrence of a breathing transverse crack in the rotor-shaft, a similar model can be adopted for them as in works [10, 11]. Namely, the stiffness matrix in (5) is periodic and its Fourier expansion can be truncated at the third harmonic component:

$$\mathbf{K}_a(\Omega t) = \mathbf{K}_{av} + \Delta \mathbf{K}_1 e^{j(\Omega t - \Theta_1)} + \Delta \mathbf{K}_2 e^{j(2\Omega t - \Theta_2)} + \Delta \mathbf{K}_3 e^{j(3\Omega t - \Theta_3)}, \quad (6f)$$

where \mathbf{K}_{av} is the coupling inner anisotropy average term, $\Delta \mathbf{K}_l, l=1,2,3$, are the stiffness matrix fluctuation components to be determined by means of the multi-fault identification. Owing to this, it will be possible to determine the amplitudes and phase angles of stiffness fluctuation caused by the inner anisotropy of the couplings.

7. Pulsation of the working medium

As mentioned above, incorrectly set stagger angles of selected blades of the blower rotor can cause unfavorable pulsation of the working medium pressure. In the case of a huge overhung rotor of the tested blower with a relatively large diameter of more than 4 m, this pulsation induces unbalanced bending moments acting on the rotor shaft line. When all rotor blades are set correctly, i.e., when their stagger angles are mutually the same, the pulsation of the working medium is characterized by a relatively small amplitude compared to the average pressure value with the so-called blade-passing frequency equal to $N \times \Omega$, where N denotes the number of blades in the rotor rim, as defined e.g., in [22]. However, when the stagger angle of one or more blades changes, the pulsation of the working medium pressure, and thus the unbalanced bending moment acting on the rotor-shaft, will indicate significant components of 1X, 2X, 3X, 4X and higher, depending on how many and which blades are incorrectly set up. Therefore, for the purpose of identifying this type of imperfection, a simple model was adopted in the form of an external excitation bending moment, which allows obtaining qualitatively very similar results compared to the analogous findings achieved in the work [23] using a three-dimensional FEM model of a multi-blade impeller and working chamber and a three-dimensional simulation of the working medium flow. The function describing a time course of this moment has the following form:

$$Z_P(\Omega t) = \sum_{j=1}^N A_j f_j^{MM} \left(\Omega t, (j-1)2\pi/N \right), \quad (6g)$$

where:

$$f_j \left(\Omega t, (j-1)2\pi/N \right) = \begin{cases} \sin \left(\Omega t + (j-1)2\pi/N \right) & \text{if } \sin \left(\Omega t + (j-1)2\pi/N \right) > 0, \\ 0 & \text{if } \sin \left(\Omega t + (j-1)2\pi/N \right) \leq 0, \end{cases}$$

A_j are the bending moment amplitudes per blade to be identified and the natural exponent MM is properly selected in order to obtain possibly the best similarity of fluctuation courses in time as these achieved in [23] by means of the advanced three dimensional models of the fan and flow. It should be emphasized that in the case of correct angular positioning of all blades of the rim, the following can be assumed: $A_j = A_0$ for $j = 1, 2, \dots, N$. Then, the amplitude spectrum of the respective time course $Z_P(\Omega t)$ is characterized by a single component with a frequency corresponding to the blade-passing frequency $N \times \Omega$. However, if at least one amplitude A_j is different from A_0 , the amplitude spectrum of $Z_P(\Omega \cdot t)$ will usually have numerous components with fundamental successive frequencies of 1X, 2X, 3X, ..., which results in corresponding external excitation bending moments in the analogous form as in (6f).

5 Multi-fault Identification Procedure

Since the identification tests of the blower under consideration can be carried out under steady-state operating conditions, i.e., at constant rotational speed Ω , and the effect of internal anisotropy of the couplings can be described by the external moments (6f), the modal equation of motion (5) is simplified to a typical form for a linear model subjected to harmonic loadings (6a)–(6g):

$$\mathbf{M}_0 \ddot{\mathbf{r}}(t) + \mathbf{D} \dot{\mathbf{r}}(t) + \mathbf{K} \mathbf{r}(t) = \mathbf{F}(\Omega t), \quad (7)$$

where all symbols retain their meaning as in the case of Eq. (5). Such harmonic loadings can be expressed as

$$\mathbf{F}(n\Omega t) = \mathbf{Q} + \mathbf{P}(n\Omega) \cos(n\Omega t) + \mathbf{R}(n\Omega) \sin(n\Omega t), \quad (8)$$

where vectors $\mathbf{P}(n\Omega)$, $\mathbf{R}(n\Omega)$ contain the modal components of fault excitation amplitudes, vector \mathbf{Q} contains the modal components of the rotor-shaft static gravitational load and $n = 1, 2, 3, \dots$, denotes the multiple of the synchronous frequency $1X$. Then, in order to obtain the system's harmonic response, an analytical solution of Eqs. (7) will be applied. For the above-mentioned harmonic excitation (8) the induced steady-state vibrations are also harmonic with the same multi-synchronous circular frequency $n\Omega$. Thus, the analytical solutions for the successive modal functions $\xi_m(t)$ contained in vector $\mathbf{r}(t)$ can be assumed in the following form:

$$\mathbf{r}(t) = \mathbf{G} + \mathbf{C} \cos(n\Omega t) + \mathbf{S} \sin(n\Omega t), \quad (9)$$

where vectors $\mathbf{C} = [c_1, c_2, \dots]^T$, $\mathbf{S} = [s_1, s_2, \dots]^T$ contain, respectively, the modal cosine- and sine-components of forced vibration amplitudes and vector \mathbf{G} contains the modal components of the rotor-shaft static deflection due to the gravitational load. Then, by substituting (8) and (9) into (7) one obtains the following systems of linear algebraic equations:

$$\begin{aligned} \mathbf{K} \cdot \mathbf{G} &= \mathbf{Q}, \\ (\mathbf{K} - (n\Omega)^2 \mathbf{M}_0) \cdot \mathbf{C} + n\Omega \cdot \mathbf{D} \cdot \mathbf{S} &= \mathbf{P}(n\Omega), \\ (\mathbf{K} - (n\Omega)^2 \mathbf{M}_0) \cdot \mathbf{S} - n\Omega \cdot \mathbf{D} \cdot \mathbf{C} &= \mathbf{R}(n\Omega). \end{aligned} \quad (10)$$

In these equations the unknown components of vectors \mathbf{C} , \mathbf{S} and \mathbf{G} are easy to determine if the excitation force vectors \mathbf{Q} , $\mathbf{P}(n\Omega)$ and $\mathbf{R}(n\Omega)$ are known. However, the target of this work is to solve the inverse problem, i.e., to determine the modal components of fault excitation amplitudes contained in vectors $\mathbf{P}(n\Omega)$ and $\mathbf{R}(n\Omega)$ based on the dynamic response of the real system under study registered by measurements. It should be noted here that the first Eq. (10) determines the static component of the system response caused by the action of constant gravitational forces only. This response can be further treated as a reference in relation to the harmonically oscillating responses which are determined by solving the second and third Eqs. (10). Therefore, achieving such a goal comes down to solving Eqs. (10)₂ and (10)₃, in which the left-hand sides should be treated as known and the right-hand sides as unknown. Since in the proposed multi-fault identification method all imperfections are described by means of external excitation forces and moments contained in vectors $\mathbf{P}(n\Omega)$ and $\mathbf{R}(n\Omega)$, and owing to this all components of matrices \mathbf{M}_0 , \mathbf{D} and \mathbf{K} matrix can be considered known, in the first step, it is necessary to determine the components of vectors \mathbf{C} and \mathbf{S} based on the measurement results.

Let us assume that in the actual rotor-shaft system of the tested machine there are M measurement points, usually located on the housings of the bearing supports. When measurements are typically taken in the horizontal "H" and vertical "V" direction at these

points, monitoring is carried out with $2M$ simultaneous diagnostic signals. Then, each of these signals can be expanded into a series with respect to orthogonal eigenfunctions of the hybrid dynamic model of the object under study in accordance with the Fourier Solution (4):

$$\varphi_m^H(t) \cong \sum_{i=1}^{2M} W_{im} \zeta_i(t) \quad \text{and} \quad \varphi_m^V(t) \cong \sum_{i=1}^{2M} U_{im} \zeta_i(t), \quad m = 1, 2, \dots, M, \quad (11)$$

where $W_{im} = W_i(x_m)$ and $U_{im} = U_i(x_m)$ denote the numerical values of respectively horizontal and vertical components of system eigenfunctions in the measurement point with the spatial coordinate of x_m . In turn, in the case of periodic dynamic responses of the monitored object caused by the above-mentioned types of imperfections, each harmonic component of the temporarily unknown modal time function $\zeta_i(t) = \zeta_i(n\Omega t)$ can be expressed in the form of:

$$\zeta_i(n\Omega t) = c_i \cos(n\Omega t) + s_i \sin(n\Omega t), \quad (12)$$

where: $i = 1, 2, \dots, 2M$, $m = 1, 2, \dots, M$ and $n = 1, 2, 3, \dots$. In an analogous way, one can express each n -th harmonic component of the dynamic response in natural coordinates measured in the horizontal ‘‘H’’ and vertical direction ‘‘V’’:

$$\begin{aligned} \varphi_m^H(n\Omega t) &= \Phi_m^H \sin(n\Omega t + \Delta_m^H) = \alpha_m^H \cos(n\Omega t) + \beta_m^H \sin(n\Omega t) \\ \text{and} \quad \varphi_m^V(n\Omega t) &= \Phi_m^V \sin(n\Omega t + \Delta_m^V) = \alpha_m^V \cos(n\Omega t) + \beta_m^V \sin(n\Omega t), \end{aligned} \quad (13)$$

where: $\Phi_m^D = \sqrt{(\alpha_m^D)^2 + (\beta_m^D)^2}$, $\Delta_m^D = \text{arc tg}(\alpha_m^D / \beta_m^D)$, $D = H, V$, $m = 1, 2, \dots, M$.

It should be emphasized here that numerical values of the amplitudes α_m^D , β_m^D or Φ_m^D can be easily determined on the basis of the results of the FFT analysis of the measured time signals. Then, considering α_m^D and β_m^D , $D = H, V$, as known, upon substituting (12) into (11), and then equating the corresponding signals in (11)–(13), the following two systems of algebraic equations are obtained by means of the harmonic balance method:

$$\mathbf{V} \cdot \mathbf{C} = \mathbf{A} \quad \text{and} \quad \mathbf{V} \cdot \mathbf{S} = \mathbf{B}, \quad (14)$$

where vectors $\mathbf{C} = [c_1, c_2, \dots, c_{2M}]^T$, $\mathbf{S} = [s_1, s_2, \dots, s_{2M}]^T$, $\mathbf{A} = [\alpha_1^H, \alpha_1^V, \alpha_2^H, \alpha_2^V, \dots, \alpha_M^H, \alpha_M^V]^T$, $\mathbf{B} = [\beta_1^H, \beta_1^V, \beta_2^H, \beta_2^V, \dots, \beta_M^H, \beta_M^V]^T$ and the $2M \times 2M$ matrix \mathbf{V} contains numerical values of the eigenfunction imaginary parts W_{im} , i.e., corresponding to the horizontal direction, in its successive odd rows and numerical values of the eigenfunction real parts U_{im} , i.e., corresponding to the vertical direction, in its successive even rows, $i = 1, 2, \dots, 2M$, $m = 1, 2, \dots, M$. In this way, separately for each n -th harmonic component of the monitored dynamic response, by solving both Eqs. (14), it is possible to experimentally determine $2M$ components of vectors \mathbf{C} and \mathbf{S} in Eqs. (10)₂ and (10)₃ corresponding to the $2M$ first eigenmodes of natural vibrations of the blower rotor-shaft system being tested. Next, by substituting them into these equations, their left-hand side values P_i^L and R_i^L , $i = 1, 2, \dots, 2M$, can be determined and contained respectively in vectors $\mathbf{P}^L(n\Omega)$ and $\mathbf{R}^L(n\Omega)$.

It should be noted that the all external excitations (6a)–(6g) resulting from the types of imperfections considered can be presented uniformly as:

$$T_k^H(t) = T_{0k} \cos(n\Omega t - \theta_k), \quad T_k^V(t) = T_{0k} \sin(n\Omega t - \theta_k), \quad k = 1, 2, \dots, K, \quad (15)$$

where T_{0k} and θ_k denote respectively the corresponding amplitudes and their phase angles, as defined in the successive relationships (6), and K is the total number of imperfections simultaneously sought by means of the proposed multi-fault identification procedure. These excitations are contained in vector $\mathbf{F}(\Omega t)$ of the system of modal equations of motion (7), where the successive components of this vector have the form of following sums with components properly weighted by the modal coefficients following from dynamic properties of the real system:

$$F_i(t) = \sum_{k=1}^K \left(\tilde{W}_{ik} T_k^H(t) + \tilde{U}_{ik} T_k^V(t) \right), \quad i = 1, 2, \dots \quad (16)$$

where respectively for the horizontal and vertical direction $\tilde{W}_{ik} = \tilde{W}_i(x_k)$ and $\tilde{U}_{ik} = \tilde{U}_i(x_k)$ denote the modal weight coefficients which are equal to: the modal displacements, i.e., $\tilde{W}_{ik} = W_i(x_k) = W_{ik}$ and $\tilde{U}_{ik} = U_i(x_k) = U_{ik}$, if the k -th excitation has a form of concentrated force, as in the cases of (6a), (6d), (6f) and (6g), the derivatives of the modal displacements with respect of the rotor-shaft line spatial coordinate x , i.e., $\tilde{W}_{ik} = W'_i(x_k) = W'_{ik}$ and $\tilde{U}_{ik} = U'_i(x_k) = U'_{ik}$, if the k -th excitation has a form of concentrated bending moment, as in the case of (6c) and (6e), or the integrals of the modal displacements with respect of the spatial coordinate x , i.e., $\tilde{W}_{ik} = \int_0^l W_{ij}(x) dx$

and $\tilde{U}_{ik} = \int_0^l U_{ij}(x) dx$, when the k -th excitation has a form of uniformly distributed force along the j -th continuous macro-element of length l , as in the case of (6b). Then, taking into account formula (8), components of the external excitation vectors $\mathbf{P}(n\Omega)$ and $\mathbf{R}(n\Omega)$ in Eqs. (10)₂ and (10)₃ take the form:

$$P_i = \sum_{k=1}^K \left(\tilde{W}_{ik} T_{0k}^C - \tilde{U}_{ik} T_{0k}^S \right), \quad R_i = \sum_{k=1}^K \left(\tilde{W}_{ik} T_{0k}^S + \tilde{U}_{ik} T_{0k}^C \right), \quad (17)$$

where: $T_{0k}^C = T_{0k} \cos \theta_k$ and $T_{0k}^S = T_{0k} \sin \theta_k$, $i = 1, 2, \dots, 2M$.

Then, the successive components P_i and R_i in (17) of vectors $\mathbf{P}(n\Omega)$ and $\mathbf{R}(n\Omega)$ can be equated to the respective previously determined values P_i^L and R_i^L , $i = 1, 2, \dots, 2M$, of the left-hand sides of Eqs. (10)₂ and (10)₃ contained in vectors $\mathbf{P}^L(n\Omega)$ and $\mathbf{R}^L(n\Omega)$, which leads to the following systems of $4M$ algebraic equations, i.e.:

$$P_i = \sum_{k=1}^K \left(\tilde{W}_{ik} T_{0k}^C - \tilde{U}_{ik} T_{0k}^S \right) = P_i^L \quad \text{and} \quad R_i = \sum_{k=1}^K \left(\tilde{W}_{ik} T_{0k}^S + \tilde{U}_{ik} T_{0k}^C \right) = R_i^L, \quad (18)$$

$$i = 1, 2, \dots, 2M.$$

One should be aware that under the proposed multi-fault identification method, the number of imperfections K searched for cannot be greater than the number of simultaneously measured $2M$ vibration signals. However, often the number of these imperfections

may be smaller than the number of measured signals, i.e., $K < 2M$. In such cases, the number of unknown components in series in the relationships (17) and (18) is smaller than the total number of Eqs. (18) to be solved. The system therefore has no single solution for all the equations and similarly as in [10, 11] one has to use the least-squares approach in order to find an unambiguous solution of the identification problem that minimize the differences between the calculated and measured results of the system's dynamic response. Another alternative is to artificially increase the number of imperfections sought, e.g., in the form of usually unavoidable static unbalances, which can be applied to practically every element of the rotor-shaft system, so as to achieve $K = 2M$. Then, Eqs. (18) can be rearranged into the following matrix form:

$$\Lambda \cdot \mathbf{T} = \mathbf{\Pi}, \quad (19)$$

where vector $\mathbf{T} = [T_{01}^C, T_{02}^C, \dots, T_{0,2M}^C, T_{01}^S, T_{02}^S, \dots, T_{0,2M}^S]^T$, $\mathbf{\Pi} = [P_1^L, P_2^L, \dots, P_{2M}^L, R_1^L, R_2^L, \dots, R_{2M}^L]^T$, and the successive rows of $4M \times 4M$ matrix Λ contain:

$$\left\{ \tilde{W}_{i1}, \tilde{W}_{i1}, \dots, \tilde{W}_{i,2M}, -\tilde{U}_{i1}, -\tilde{U}_{i2}, \dots, -\tilde{U}_{i,2M} \right\}, \quad i = 1, 2, \dots, 2M,$$

and $\left\{ \tilde{U}_{i1}, \tilde{U}_{i2}, \dots, \tilde{U}_{i,2M}, \tilde{W}_{i1}, \tilde{W}_{i2}, \dots, \tilde{W}_{i,2M} \right\}, \quad i = 2M + 1, 2M + 2, \dots, 4M.$

Solving the system of Eqs. (19) separately for successive multiples of the synchronous system rotational speed nX , $n = 1, 2, 3, \dots$, we identify the amplitudes of the sought types of imperfections described by relationships (6a-g) and their phase angles, bearing in mind that: $\sqrt{(T_{0k}^C)^2 + (T_{0k}^S)^2} = T_{0k}$ and $\arctg\left(\frac{T_{0k}^S}{T_{0k}^C}\right) = \theta_k$.

6 Exemplary Results of Identification

The fundamental step in realizing the proposed model-based, multi-fault identification procedure is to determine the basic parameters of the structural hybrid model of the blower rotor-shaft system under study initially treated as free of imperfections. In this model, a total number of the continuous finite macro-elements substituting individual cylindrical segments of the real stepped shaft line, their geometrical dimensions and material constants have been set up basing on the technical documentation of the blower under study. As a result, the hybrid model of this object consists of $n = 66$ finite macro-elements. In turn, numerical values of the bearing stiffness and damping coefficients were provided by manufacturers of the individual components of the blower drive system, i.e. the blower overhung rotor-shaft and the both electric motors. To determine stiffness coefficients of the bearing housings and their foundations, the three-dimensional finite element technique was applied, the introductory results obtained using which were verified next using proper experimental tests.

As mentioned above, the entire rotor-shaft system of the tested industrial blower is suspended by 6 bearing supports. Accelerometers are installed on each of them to measure their lateral vibrations in the horizontal and vertical directions. Owing to this, $2M = 12$ signals are being recorded simultaneously during regular operation of the machine at nominal, steady-state conditions. These vibration signals in time domain are

properly filtered, integrated with regard of time, and their selected time windows are then transformed into frequency domain using the fast Fourier transformation technique (FFT). In Fig. 3 there are presented amplitude spectra of the signals measured by the sensors attached to the individual bearing supports, i.e., starting from bearing #1 in the vicinity of the blower rotor to bearing #6 at the non-driven end of the second driving motor “1” (see Fig. 1). The frequency values on the abscissa axes of plots in Fig. 3 are referred to the rotor-shaft’s nominal rotational speed, so that the most significant amplitude peaks in all these graphs correspond to successive multiples of the synchronous frequencies 1X, 2X, 3X, ... According to formula (13), each peak maximal value corresponds to the respective partial amplitudes α_m^D and β_m^D , $D = H, V$, where H denotes the horizontal direction, and V denotes the vertical direction.

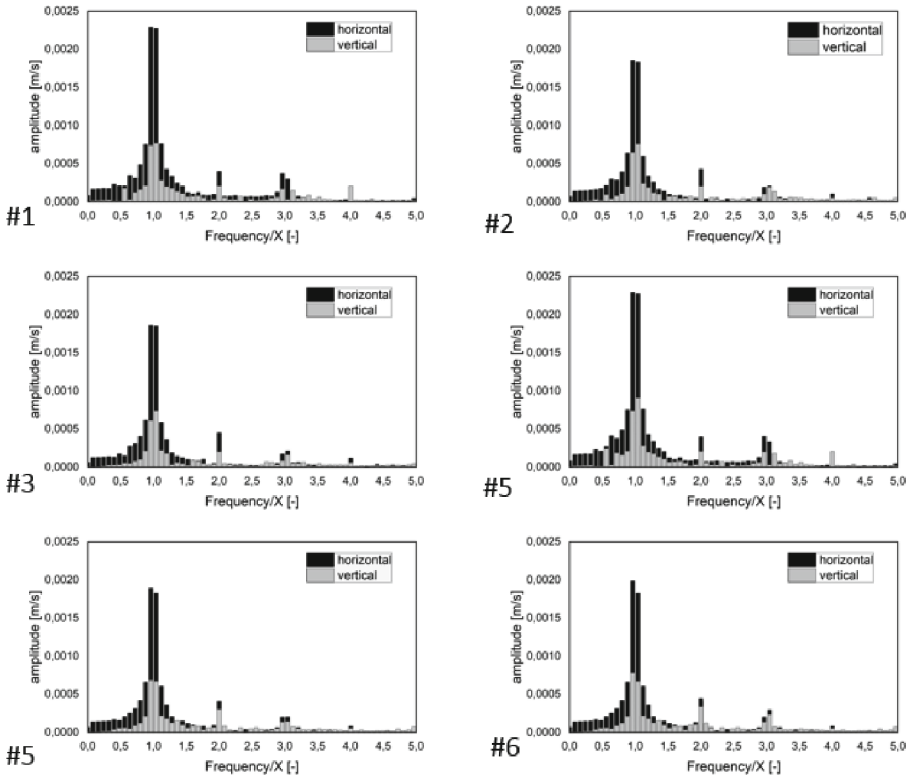


Fig. 3. Amplitude characteristics of the measured lateral vibrations at the bearing housings.

To obtain the modal response amplitudes c_i and s_i , $i = 1, 2, \dots, 2M$, as defined by Eq. (12), the components of matrix \mathbf{V} need to be determined first by means of the bending/lateral eigenvibration analysis of the blower rotor-shaft system model assumed to be free of imperfections. This goal is achieved by solving both systems of algebraic Eqs. (14).

According to the principles of the proposed model-based multi-fault identification procedure, the causes of the successive peaks 1X, 2X and 3X shown in Fig. 3 are going to

be found, where the system static response due to the gravitational loading will be used here as a reference. In the blower rotor-shaft system being tested, static unbalances of the blower overhung rotor and two electric motor rotors, dynamic unbalance of the blower rotor as well as parallel and angular misalignments of the four couplings C1, C2, C3 and C4 (see Fig. 1) are suspected to be the causes of 1X oscillation components, which are predominant in each amplitude-frequency characteristics presented in Fig. 3. Here, the total number K of these imperfections is equal to 12, what enables us to solve Eq. (19) under condition $K = 2M = 12$. Then, using expressions (6a)–(6e), parameters of these imperfections exciting the 1X vibration components can be obtained. The parameter values of these imperfections are demonstrated in Table 1. Based on the numerical values of the imperfection parameters inducing the vibration components with a frequency of 1X, it can be concluded that the vanishingly small values of β_k prove negligible angular misalignments of all four couplings in the tested system.

Table 1. Identification results for the 1X vibration components.

Blower rotor dynamic unbalance	Blower rotor static unbalance	Rotor static unbalance of Motor 1	Rotor static unbalance of Motor 2
$\alpha = 0.0653$ [deg]	$m\varepsilon = 0.592$ [kgm]	$e_1 = 1.248 \cdot 10^{-4}$ [m]	$e_2 = 0.536 \cdot 10^{-4}$ [m]
$\delta = 0.784$ [rad]	$\alpha = 0.586$ [rad]	$\beta_1 = 0.002$ [rad]	$\beta_2 = -1.912$ [rad]
Coupling C1 parallel misalignment	Coupling C2 parallel misalignment	Coupling C3 parallel misalignment	Coupling C4 parallel misalignment
$\delta_1 = 0.00051$ [m]	$\delta_2 = 0.000969$ [m]	$\delta_3 = 0.001139$ [m]	$\delta_4 = 0.000991$ [m]
$\psi_1 = 2.567$ [rad]	$\psi_2 = 4.111$ [rad]	$\psi_3 = -3.989$ [rad]	$\psi_4 = 2.753$ [rad]
Coupling C1 angular misalignment	Coupling C2 angular misalignment	Coupling C3 angular misalignment	Coupling C4 angular misalignment
$\beta_1 = 2.013 \cdot 10^{-5}$ [rad]	$\beta_2 = 7.315 \cdot 10^{-6}$ [rad]	$\beta_3 = 1.526 \cdot 10^{-4}$ [rad]	$\beta_4 = 8.004 \cdot 10^{-5}$ [rad]
$\phi_1 = 4.872$ [rad]	$\phi_2 = -0.273$ [rad]	$\phi_3 = 1.694$ [rad]	$\phi_4 = -3.116$ [rad]

In the next step of this identification procedure, parameters of imperfections responsible for excitation of the 2X oscillation components are going to be determined. These are the inner anisotropies of all couplings C1, C2, C3 and C4, and wrongly set-up stagger angles of selected blades of the blower rotor causing unfavorable pulsation of the working medium pressure, and consequently unbalanced oscillatory bending moment imposed to the rotor-shaft. Then, the number of these faults is equal to 5. However, it should be remembered that, according to the dynamic equilibrium conditions (3), the inner anisotropy of each of these couplings is affected by two unknown parameters, i.e., the fluctuation amplitudes of shear and flexural stiffness G_{V_k} and H_{V_k} , respectively. Consequently, $K = 1 + 4 \cdot 2 = 9 < 12 = 2M$. Because here a greater number of Eqs. (19) is available than the number of unknowns, the abovementioned least-square approach

had to be applied to obtain the most accurate solutions compared to those determined using the results of experimental measurements. The same approach was used to identify the 3X vibration components suspected to be induced by the same $K = 9$ parameters of imperfections. Then, as a result of inverse Fourier transformation of expression (6f), amplitudes of bending stiffness fluctuation due to the inner anisotropy of the four couplings as well as rates of the stagger angles of two blades in the blower rotor have been determined. Numerical values of the fluctuation amplitudes of shear and flexural stiffness G_{V_k} and H_{V_k} , $k = 1, 2, 3, 4$, are contained in Table 2. Comparing these stiffness values shows that G_{V_k} and H_{V_k} for $k = 1, 2, 3$ are much smaller than G_{V_4} and H_{V_4} . This means that only coupling C4 (see Fig. 1) indicates a noticeable internal anisotropy. In turn, the determined amplitudes of time-histories of the unbalanced bending moment caused by excessive fluctuations of the pressure of the blower working medium have shown wrong stagger angles of two opposite blades out of a total of 20 blades in the rotor rim, as a result of which the flow rate for these two blades decreased by approximately half.

Table 2. Identification results for the 2X vibration components.

Coupling C1 shear stiffness fluct. ampl.	Coupling C2 shear stiffness fluct. ampl.	Coupling C3 shear stiffness fluct. ampl.	Coupling C4 shear stiffness fluct. ampl.
$G_{V1} = 5.1 \cdot 10^5$ [N/m]	$G_{V2} = 1.13 \cdot 10^4$ [N/m]	$G_{V3} = 7.81 \cdot 10^4$ [N/m]	$G_{V4} = 3.75 \cdot 10^7$ [N/m]
$\Delta_1 = 2.742$ [rad]	$\Delta_2 = -3.251$ [rad]	$\Delta_3 = -1.001$ [rad]	$\Delta_4 = 5.135$ [rad]
Coupling C1 bending stiffness fluct. ampl.	Coupling C2 bending stiffness fluct. ampl.	Coupling C3 bending stiffness fluct. ampl.	Coupling C4 bending stiffness fluct. ampl.
$H_{V1} = 3.12 \cdot 10^6$ [Nm/rad]	$H_{V2} = 6.01 \cdot 10^5$ [Nm/rad]	$H_{V3} = 9.73 \cdot 10^6$ [Nm/rad]	$H_{V4} = 5.04 \cdot 10^8$ [Nm/rad]
$\Gamma_1 = -1.783$ [rad]	$\Gamma_2 = 2.124$ [rad]	$\Gamma_3 = 4.944$ [rad]	$\Gamma_4 = -0.626$ [rad]

Finally, in order to verify an accuracy of the results of the multi-fault identification procedure, and in this way to compare the real and identified fault parameters, a numerical simulation of bending/lateral vibrations of the hybrid model of the blower rotor-shaft system has been performed, taking into consideration simultaneous interactions of the all imperfections considered above. In Fig. 4 there are plotted time histories of the horizontal and vertical vibration velocities of the six bearing housings #1 – #6 obtained theoretically by solving Eqs. (5) and experimentally, where the amplitude-frequency spectra of these measured ones are presented in Fig. 3. From the comparison of the respectively corresponding plots a fairly good similarity of the measured and calculated results is visible. This proves a reliability of the proposed model-based multi-fault identification procedure proposed in this paper. It should be noted that the vibration velocity waveforms obtained both experimentally and computationally, especially in the case of bearing housings #3–#6 supporting both drive motors, are characterized by an additional relatively fast-fluctuating component with a frequency of 100 Hz caused by the typical magnetic pull of the rotors of these motors.

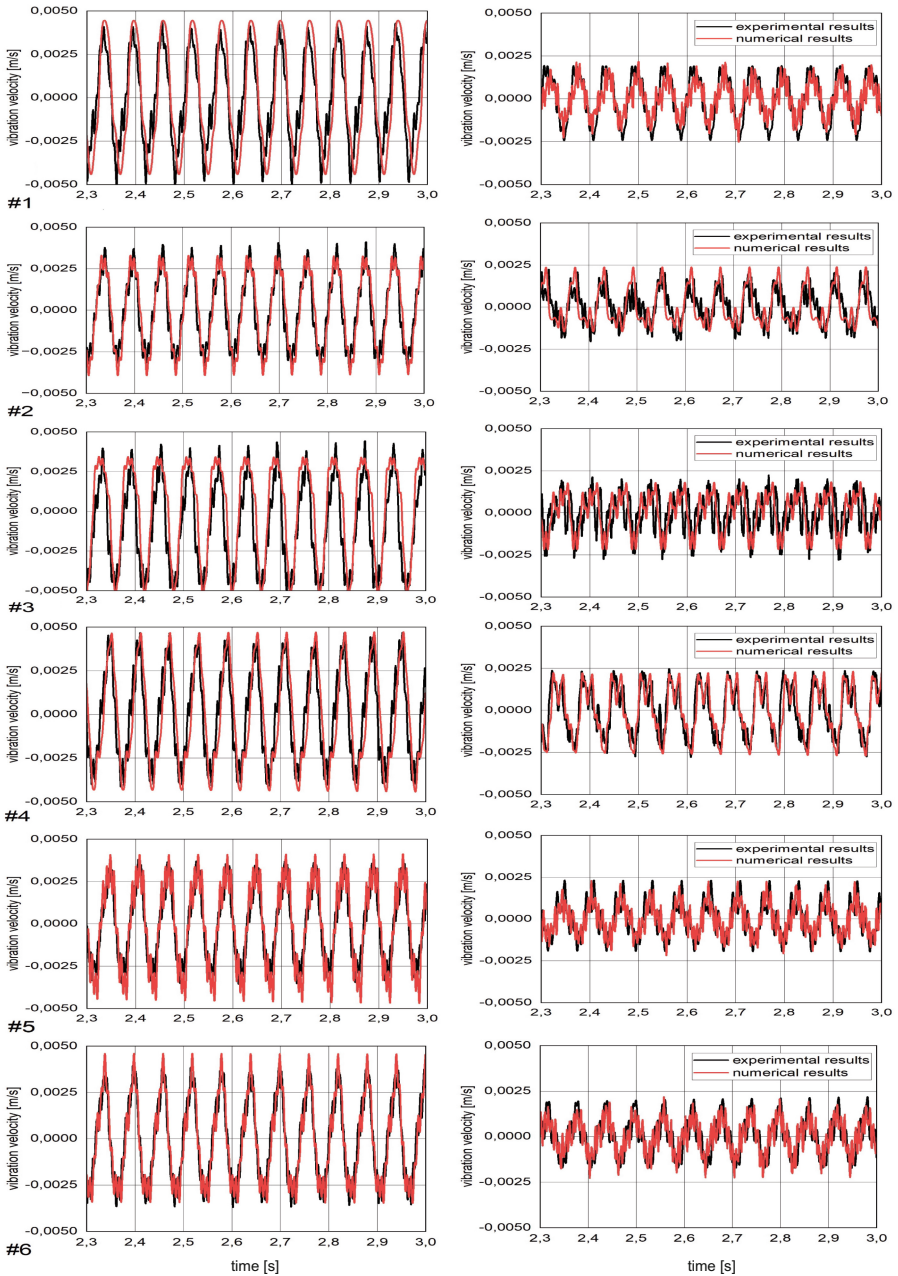


Fig. 4. Measured and simulated horizontal (left column) and vertical (right column) vibration velocities at the bearing supports #1–#6.

7 Final Remarks

The paper proposes a multi-fault identification method for rotating machines based on a structural continuous finite macro-element model of the tested object. In this method, the maximum number of simultaneously identified, the most probable imperfections is limited to the number of courses of lateral/bending vibrations simultaneously monitored on a real object. Here, subsequent peaks of the amplitude spectra of measured dynamic responses of the real object are the basis for determination of parameters of individual types of system's imperfections with frequencies respectively corresponding to these peaks. In this paper, there were identified residual static and dynamic unbalances, parallel and angular misalignments and local inner anisotropies affecting simultaneously the rotor shaft system of the high-power blower used in the mining industry. Their mutual contributions within the numerical values of the amplitudes of the respective peaks of the frequency spectra recorded by individual sensors result from system's sensitivity to the excitations caused by these imperfections, which was determined by the modal description of motion of the model of the tested object. Moreover, by means of this method wrong stagger angles of the two opposing blades in the rim of the blower rotor, which resulted in additional lateral/bending vibration components, were detected. It should be emphasized that the practical efficiency and accuracy of the proposed method depends on the credibility of the theoretical model of the rotor-shaft system of the tested machine as well as on sampling densities of the measured signals and the accuracy of FFT analyses performed for them.

References

1. Childs, D.: *Turbomachinery Rotordynamics: Phenomena, Modeling, and Analysis*. Wiley (1993). ISBN: 978-0-471-53840-0
2. Genta, G.: *Dynamics of Rotating Systems*. Springer US, New York, NY (2005)
3. Al-Hussain, K.M., Redmond, I.: Dynamic response of two rotors connected by rigid mechanical coupling with parallel misalignment. *J. Sound Vib.* **249**(3), 483–498 (2002)
4. Al-Hussain, K.M.: Dynamic stability of two rigid rotors connected by a flexible coupling with angular misalignment. *J. Sound Vib.* **266**, 217–234 (2002)
5. Lees, A.W.: Misalignment in rigidly coupled rotors. *J. Sound Vib.* **305**, 261–271 (2007)
6. Redmond, I.: Study of a misaligned flexibly coupled shaft system having nonlinear bearings and cyclic coupling stiffness – Theoretical model and analysis. *J. Sound Vib.* **329**, 700–720 (2010)
7. Didier, J., Sinou, J.-J., Faverjon, B.: Study of the non-linear dynamic response of a rotor system with faults and uncertainties. *J. Sound Vib.* **331**, 671–703 (2012)
8. Pennacchi, P., Vania, A., Chatterton, S.: Nonlinear effects caused by coupling misalignment in rotors equipped with journal bearings. *Mech. Syst. Signal Process.* **30**, 306–322 (2012)
9. Malta, J.: Investigation of anisotropic rotor with different shaft orientation. Doctoral Thesis, Darmstadt University of Technology, Department of Machinery Construction, D 17, Darmstadt (2009)
10. Bachschmid, N., Pennacchi, P., Vania, A.: Identification of multiple faults in rotor systems. *J. Sound Vib.* **254**(2), 327–366 (2002)
11. Pennacchi, P., Bachschmid, N., Andrea Vania, A., Zanetta, G.A., Gregorib, L.: Use of modal representation for the supporting structure in model-based fault identification of large rotating machinery: part I—theoretical remarks. *Mech. Syst. Signal Process.* **20**, 662–681 (2006)

12. Szolc, T., Tazowski, P., Stocki, R., Knabel, J.: Damage identification in vibrating rotor-shaft systems by efficient sampling approach. *Mech. Syst. Signal Process.* **23**, 1615–1633 (2009)
13. Szolc, T., Tazowski, P., Stocki, R., Knabel, J.: Nonlinear and parametric coupled vibrations of the rotor-shaft system as fault identification symptom using stochastic methods. *Nonlinear Dyn.* **57**, 533–557 (2009)
14. Szolc, T., Konowrocki, R.: Research on stability and sensitivity of the rotating machines with overhung rotors to lateral vibrations. *Bull. Polish Acad. Sci. Tech. Sci.* **69**(6), e137987 (2021)
15. Isermann, R.: Model-based fault detection and diagnosis – status and applications. In: *Proceedings of Automatic Control in Aerospace*, pp 49–60. Elsevier IFAC Publications, Saint-Petersburg, Russia (2004)
16. Lees, A.W., Sinha, J.K., Friswell, M.I.: Model-based identification of rotating machines. *Mech. Syst. Signal Process.* **23**, 1884–1893 (2009)
17. Bachschmid, N., Pennacchi, P., Vania, A.: Use of modal representation for the supporting structure in model based fault identification of large rotating machinery: part 2 – application to a real machine. *Mech. Syst. Signal Process.* **20**(3), 682–701 (2006)
18. Lal, M., Tiwari, R.: Multi-fault identification in simple rotor-bearing-coupling systems based on forced response measurements. *Mech. Mach. Theory* **51**, 87–109 (2012)
19. Harish Chandra, N., Sekhar, A.S.: Fault detection in rotor bearing systems using time frequency techniques. *Mech. Syst. Signal Process.* **72–73**, 105–133 (2016)
20. El-Mongy, H.H., Younes, Y.K.: Vibration analysis of a multi-fault transient rotor passing through subcritical resonances. *J. Vib. Control* **24**(14), 2986–3009 (2018)
21. Szolc, T.: On the discrete-continuous modeling of rotor systems for the analysis of coupled lateral-torsional vibrations. *Int. J. Rotating Mach.* **6**(2), 135–149 (2000)
22. Xie, F., Li, Z., Ganeriwala, S.: *Vibration signal analysis of fan rotors*. Technote, SpectraQuest Inc. SQi-14A-052007 (2007)
23. Ye, X., Ding, X., Zhang, J., Li, C.: Numerical simulation of pressure pulsation and transient flow field in an axial flow fan. *Energy* **129**, 185–200 (2017)